Heat Transfer to Axisymmetric Bodies in Super- and Hypersonic Turbulent Streams

A. T. Wassel*
Spectron Development Laboratories, Costa Mesa, Calif.
and
V. E. Denny†
University of California at Los Angeles, Los Angeles, Calif.

An analysis of the effects of freestream turbulence on heat and momentum transfer to axisymmetric bodies in super- and hypersonic turbulent streams has been performed. Real air density, viscosity, and Prandtl number were taken variable across the boundary layer. Results were obtained for a range of freestream Mach number, total pressure, total temperature, and intensity of turbulence, as well as wall temperature. The results confirm previous findings that heat transfer to the surface can be enhanced markedly by turbulence in the freestream, the effect being more pronounced at lower Mach numbers and higher total pressures. The magnification in heat transfer is less pronounced at higher total temperature and lower wall temperature as a result of variable property effects. In arc-heated jet facilities environments, freestream turbulence is shown to be a major contributor to the so-called enthalpy spike. Discrepancies between enthalpies inferred from null point calorimeters and those derived from system overall energy balances are predicted.

Nomenclature

A_D, A_μ = dissipation and viscosity constants, respectively
C = viscosity-density ratio $\rho\mu/\rho_e\mu_e$
C_D, C_μ = dissipation and viscosity constants, respectively
C_f = skin friction coefficient
D = model diameter
DF = damping factor
f = dimensionless stream function
h = fluid enthalpy
H = dimensionless enthalpy h/h_e
I = density integral
l_D, l_μ = dissipation and viscosity length scales, respectively
P = pressure
Pr = Prandtl number
q = kinetic energy of turbulence
$\dot{q}_c''$ = convective heat flux
Q = dimensionless kinetic energy of turbulence
r = local body radius
R = $\rho q^{1/2} y/\mu$
Re = Reynolds number
t = temperature
T = turbulence intensity $\sqrt{u'^2_\infty}/V_\infty$
u, v = velocity components in streamwise and normal directions
V_∞ = freestream velocity
x, y = streamwise and normal coordinates
β = pressure gradient coefficient
η = transformed coordinate normal to the surface
μ = fluid dynamic viscosity
ρ = fluid density
ξ = transformed coordinate along the surface
τ = shear stress
ψ = stream function

Subscripts

D = diameter
e = edge of the boundary layer
eff = effective = laminar + turbulent
h = enthalpy
q = kinetic energy of turbulence
t = turbulent, total
w = wall
x = streamwise
∞ = freestream

Received Feb. 13, 1976; revision received Nov. 29, 1976.
Index categories: Boundary Layers and Convective Heat Transfer – Laminar; Boundary Layers and Convective Heat Transfer – Turbulent; Supersonic and Hypersonic Flow.
*Staff Scientist. Member AIAA.
†Associate Professor.

Introduction

ARC-HEATED jet facilities, as a means for producing high-pressure/high-enthalpy flows, have been in use and under development for several years. Such facilities have been utilized as material and concept screening devices and, recently, for extracting surface roughness, transition, and shape change data.

Unfortunately, arc-heated jets inherently involve severe flow characteristics that introduce exceptional difficulties in the measurement and calibration of flow parameters. Because of the severity of the external environment, calibration is performed using null-point heat-transfer calorimeters and pressure probes in the sweeping mode. The flow enthalpy then is derived from averaged heat-transfer and pressure profiles, applying any suitable standard laminar stagnation-point heat-transfer theory, e.g., Fay and Riddell.[1] However, it has been observed that these *inferred* enthalpies are substantially larger than bulk enthalpies derived from an overall system energy balance.[2] Freestream turbulence in the arc flow has been identified as a possible cause for this flow anomaly. The purpose of the present study is to investigate the effects of freestream turbulence (velocity fluctuations) on heat and momentum transfer to axisymmetric bodies in super- and hypersonic streams.

Although very little work has been carried out for high-speed flows, considerable effort has been addressed to subsonic flows. Kestin[3] presented a good review article on the effects of freestream turbulence on heat transfer associated with bluff bodies and flat plates. Hsu and Sage[4] measured local transport from spheres in turbulent environments.

Venezian et al.[5] measured thermal and material transfer between turbulent gas streams and 1-in. spheres and showed that the Nusselt number decreased with increasing angle up to the separation point. The results imply that boundary-layer transition failed to occur and that the flow was fully turbulent. Kestin[3] also showed that the Froessling number for a cylinder in cross flow increases on increasing the turbulence intensity, again implying the absence of boundary-layer transition. Gardon and Akfirat[6,7] measured local as well as average heat transfer between isothermal flat plates and impinging two-dimensional jets. They showed that artificial increases in the jet turbulence yielded not only higher stagnation-point heat transfer but fully turbulent boundary layers as well. Lavender and Pei[8] investigated experimentally the effect of turbulence on overall heat transfer from spheres. Gostowski and Cotello[9] reported experimental data for the effect of freestream turbulence on heat transfer at the stagnation point of a sphere.

Modeling the mechanisms that produce these anomalies has assumed two different approaches in the literature. For an incompressible flow, Smith and Kuethe[10] modeled the effect as a turbulent transfer superposed on a laminar one. Their turbulence model involved an eddy viscosity that is proportional to freestream turbulence and distance from the wall. Galloway[11] represented the eddy viscosity in terms of the law of the wall ($\mu_t \sim y$) and by a roll cell mechanism ($\mu_t \sim y^3$). Traci and Wilcox,[12] adopting Saffman's turbulence model, studied the effect of freestream turbulence on stagnation-point flow and heat transfer for an incompressible constant property flow. Recently, Wassel and Denny,[13] introducing a conservation equation for the kinetic energy of the fluctuating velocity components, investigated the effects of freestream turbulence on heat and momentum transport to axisymmetric bodies in subsonic streams.

An alternative approach to simulating freestream-turbulence/boundary layer interactions was considered by Sutera et al.,[14] Sutera,[15] and Weeks.[16] They studied the effect of freestream turbulence on stagnation zone transport phenomena via the mechanism of vorticity stretching and showed that stagnation skin friction and heat transfer increase as a result of specifically oriented upstream steady vorticity fields convected through the boundary layer. However, the flow configurations in Refs. 14-16 can be viewed as oversimplifications of the actual flow on taking cognizance of the stochastic nature of the turbulent fluctuating velocity components.

For super- and hypersonic flows, Weeks[16] found that a specifically oriented upstream vorticity can be amplified in the boundary layer if the turbulence wavelength is greater than a neutral value. For wavelengths smaller than the neutral, the imposed freestream vorticity will attenuate. Weeks presented heat-transfer enhancement in terms of a turbulence amplitude parameter and an Eckert number.

The objective of the present work is to predict heat- and momentum-transfer enhancement in the stagnation region of axisymmetric bodies owing to turbulence in otherwise laminar super- and hypersonic streams. Real air data for density, viscosity, and Prandtl number are applied across the boundary layer in terms of curve fits involving static enthalpy ratios. The boundary layer is assumed to be fully turbulent. The process visualized is one wherein turbulence in the boundary layer results from penetration of freestream fluid eddies. The kinetic energy of the fluctuating velocity components is assumed to be governed by a conservation equation that accounts for advection, diffusion, decay, and generation mechanisms of turbulence. Turbulence can be generated by shear if the velocity gradient is nonzero. The practical objective is to quantify freestream turbulence effects in a form that can be incorporated readily in engineering applications.

Analysis

Governing Equations and Turbulence Model

Boundary-layer forms of the conservation equations for a compressible turbulent, axisymmetric flow are taken as

$$\frac{\partial}{\partial x}(\rho u r) + \frac{\partial}{\partial y}(\rho v r) = 0 \tag{1}$$

$$\rho u \frac{\partial u}{\partial x} + \rho v \frac{\partial u}{\partial y} = -g_0 \frac{dP}{dx} + \frac{\partial}{\partial y}\left(\mu_{\text{eff}} \frac{\partial u}{\partial y}\right) \tag{2}$$

$$\rho u \frac{\partial h}{\partial x} + \rho v \frac{\partial h}{\partial y} = \frac{\partial}{\partial y}\left(Pr_{h,\text{eff}}^{-1} \mu_{\text{eff}} \frac{\partial h}{\partial h}\right) + \frac{\mu_{\text{eff}}}{g_0 J}\left(\frac{\partial u}{\partial y}\right)^2 + \frac{u}{J}\frac{dP}{dx} \tag{3}$$

where μ_{eff} and $Pr_{h,\text{eff}}$ incorporate laminar and turbulent contributions to the transfer coefficients, that is

$$\mu_{\text{eff}} = \mu + \mu_t \tag{4}$$

$$Pr_{h,\text{eff}} = \mu_{\text{eff}} / (\mu Pr^{-1} + \mu_t Pr_t^{-1}) \tag{5}$$

Following Refs. 17-19, the turbulent eddy viscosity is obtained via a conservation equation of the Kolmogorov-Prandtl type wherein the kinetic energy q of the fluctuating velocity components is assumed to be governed by a rate equation. The eddy viscosity is related to q through a viscosity length scale l_μ, which, in turn, is a function of the local velocity fluctuations $q^{1/2}$. The kinetic energy of turbulence rate equation assumes the form

$$\rho u \frac{\partial q}{\partial x} + \rho v \frac{\partial q}{\partial y} = \frac{\partial}{\partial y}\left(Pr_{q,\text{eff}}^{-1} \mu_{\text{eff}} \frac{\partial q}{\partial y}\right) + \mu_t \left(\frac{\partial u}{\partial y}\right)^2 - \frac{C_D \rho q^{3/2}}{l_D} \tag{6}$$

where

$$Pr_{q,\text{eff}} = \mu_{\text{eff}} / (\mu + \mu_t Pr_q^{-1}) \tag{7}$$

Table 1 Laminar flow results ($P_{t,\infty}$ = 35, 75 atm)

H_w	t_w, °R	$Nu_w/Re_w^{1/2}$ This study	$Nu_w/Re_w^{1/2}$ Fay-Riddel	$Nu_w/Re_w^{1/2}$ Cohen	$Nu_e/Re_e^{1/2}$	$C_f/2(x/D)Re_e^{1/2}$
0.9	540	0.6576	0.6526	0.6572	0.663	1.261
	1500	0.6519	0.6529	0.6515	0.669	1.286
0.75	540	0.6405	0.6358	0.6388	0.657	1.197
	1500	0.6328	0.6363	0.6338	0.682	1.249
0.5	540	0.6078	0.5998	0.6001	0.660	1.118
	1500	0.5899	0.6012	0.5962	0.729	1.190
0.2	540	0.5331	0.5269	0.5222	0.742	1.069
	1500	0.5033	0.5294	0.5200	0.740	1.131
0.1	540	0.4712	0.4784	0.4707	0.774	1.072
	1500	0.4522	0.4813	0.4694	0.719	1.118

$$\mu_t = C_\mu \rho q^{1/2} l_\mu \tag{8}$$

Equations (6-8) yield the eddy viscosity distribution across the boundary layer. The dissipation and viscosity length scales are represented by empirical algebraic expressions in a fashion similar to Prandtl mixing length theory[20] and are assumed to be proportional to the distance from the wall in the turbulent core and to $yR \sim y^2 q^{1/2}$ in the sublayer.[18,21] Thus, l_D and l_μ are expressed by

$$l_D = y[1 - \exp(-A_D R)] \tag{9}$$

$$l_\mu = y[1 - \exp(-A_\mu R)] \tag{10}$$

where

$$R = q^{1/2} y \rho / \mu \tag{11}$$

The preceding set of equations is subject to the boundary conditions

$$u = v = 0, \quad h = h_w, \quad q = 0 \tag{12a}$$

at $y = 0$, and

$$u = u_e, \quad h = h_e, \quad q = q_e \tag{12b}$$

as $y \to \infty$. The quantity q_e is the kinetic energy of the velocity fluctuations at the edge of the boundary layer, its magnitude being related to the freestream turbulence, as will be shown.

Thermophysical Properties

The fluid considered is real air with variable density, viscosity, and Prandtl number. Following Refs. 22-24, the density, density-viscosity ratio, and Prandtl number are given by

$$\frac{\rho}{\rho_e} = \frac{(h_e/h_{\text{ref}})^{0.6123} - 0.0455283}{(h/h_{\text{ref}})^{0.6123} - 0.0455283} \tag{13}$$

$$\frac{\rho\mu}{\rho_e \mu_e} = \frac{(h_e/h_{\text{ref}})^{0.3329} - 0.020856}{(h/h_{\text{ref}})^{0.3329} - 0.020856} \tag{14}$$

$$Pr = Pr_1 + \sum_{n=1}^{N} a_n \left(\frac{h}{h_{\text{ref}}} - Pr_2 \right)^n \tag{15}$$

where h_{ref} is a reference enthalpy, and the quantities Pr_1, Pr_2, a_n, and N depend on h/h_{ref}.

Governing Equations in Self-Similar Form

Introducing standard Levy-Lees' coordinates (ξ, η)

$$\xi = \int_0^x \rho_e \mu_e u_e r^2 \, dx \tag{16}$$

$$\eta = \frac{\rho_e u_e r}{(2\xi)^{1/2}} \int_0^y \frac{\rho}{\rho_e} dy \tag{17}$$

and stream functions ψ and f

$$\rho u r = \partial\psi/\partial y, \quad \rho v r = -(\partial\psi/\partial x), \quad \psi = (2\xi)^{1/2} f$$

into the governing differential equations,

$$\frac{\partial}{\partial\eta}\left(C_{\text{eff}} \frac{\partial^2 f}{\partial\eta^2} \right) + f\frac{\partial^2 f}{\partial\eta^2} + \beta\left[\left(\frac{\rho_e}{\rho} \right) - \left(\frac{\partial f}{\partial\eta} \right)^2 \right] = 0 \tag{18}$$

$$\frac{\partial}{\partial\eta}\left(C_{\text{eff}} Pr^{-1}_{h,\text{eff}} \frac{\partial H}{\partial\eta} \right) + f\frac{\partial H}{\partial\eta} = 0 \tag{19}$$

$$\frac{\partial}{\partial\eta}\left(C_{\text{eff}} Pr^{-1}_{q,\text{eff}} \frac{\partial Q}{\partial\eta} \right) + f\frac{\partial Q}{\partial\eta} - \frac{C_D Q^{3/2}}{[I(\eta) DF_D]} = 0 \tag{20}$$

where

$$C_{eff} = \frac{\mu_{\text{eff}}}{\mu_e}\frac{\rho}{\rho_e} = \left(\frac{\mu_t}{\mu_e} + \frac{\mu}{\mu_e} \right)\frac{\rho}{\rho_e} \tag{21a}$$

$$\beta = \frac{2\xi}{u_e}\frac{du_e}{d\xi} = \frac{1}{2}, \qquad \frac{u}{u_e} = \frac{\partial f}{\partial\eta} \tag{21b}$$

$$H = \frac{h}{h_e}, \quad Q = \frac{q}{\mu_e (du_e/dx)/\beta\rho_e} \tag{21c}$$

$$I(\eta) = \int_0^\eta \left(\frac{\rho_e}{\rho} \right) d\eta, \quad DF_D = [1 - \exp(-A_D R)] \tag{21d}$$

$$\frac{\mu_t}{\mu_e} = C_\mu \left(\frac{\mu}{\mu_e} \right) DF_\mu R, \quad DF_\mu = [1 - \exp(-A_\mu R)] \tag{21e}$$

$$R = \left(\frac{\rho}{\rho_e} \right)\left(\frac{\mu_e}{\mu} \right) I(\eta) Q^{1/2} \tag{21f}$$

Equations (18-20) are subject to the boundary conditions

$$f = -\frac{\partial f}{\partial\eta} = 0, \quad H = H_w, \quad Q = 0 \tag{22a}$$

at $\eta = 0$, and

$$\partial f/\partial\eta = 1, \quad H = 1, \quad Q = Q_e \tag{22b}$$

as $\eta \to \infty$ and may be solved approximately by various methods. The wall fluxes for momentum and energy transport then may be represented in terms of the dimensionless edge kinetic energy of turbulence Q_e and the enthalpy ratio across the boundary layer H_w. It will be shown below that the freestream conditions and those behind a normal shock can be absorbed in H_w and Q_e and the governing set of equations then solved parametrically. Self-similar forms of the governing differential equations are valid in the region of interest. Heat-transfer data around spheres in turbulent environments[3,4] show that the wall heat flux drops only slightly up to angles of approximately 25° (stagnation point being at 0°.)

Relation Among Q_e, Reynolds Number, and Freestream Turbulence

The boundary-layer edge Q_e is related to the freestream intensity of turbulence, $T = \sqrt{u_e'^2}/V_\infty$, by the following definitions

$$Q_e = \tfrac{3}{4} T^2 \left[\frac{\rho_e V_\infty^2}{\mu_e du_e/dx} \right] \tag{23}$$

or

$$Q_e = \tfrac{3}{4} T^2 (Re^2_{D,\infty}/Re_{D,e})(\rho_e/\rho_\infty)^2 (\mu_\infty/\mu_e)^2 \tag{24}$$

The Reynolds numbers $Re_{D,\infty}$ and $Re_{D,e}$ are defined by

$$Re_{D,\infty} = \rho_\infty V_\infty D/\mu_\infty, \quad Re_{D,e} = \rho_e du_e/dx \, D^2/\mu_e \tag{25}$$

The turbulence intensity is defined relative to the freestream velocity. The density and viscosity ratios in Eq. (24) are those that apply across a normal shock.

In the foregoing, the tangential fluctuating velocity component was assumed to be invariant across the shock. This assumption is, of course, questionable, and a study is needed to determine what happens to the turbulent components as they cross the shock and propagate along a streamline to the edge of the boundary layer. However, if the value of the fluctuating component does change across the shock, the analysis remains unchanged, with the value of Q_e being multiplied by a correction factor.

The velocity gradient du_e/dx is obtained from Euler's equation and the pressure distribution around the body. The dimensionless kinetic energy of turbulence at the boundary-layer edge, defined by Eq. (23) or (24), is a function of the freestream turbulent fluctuations and the stagnation region density, viscosity, and velocity gradient. The latter quantities depend on freestream conditions and properties across the shock. Equation (23) or (24) therefore can be rewritten as follows

$$Q_e = Q_e(\overline{u_\infty'^2},\ M_\infty,\ P_{t,\infty},\ h_t, D) \tag{26}$$

It is seen from Eq. (26) that freestream conditions as well as those behind a normal shock can be absorbed in the definition for Q_e.

Auxiliary Relations

In order to predict transfer rates for specific flow conditions, i.e., M_∞, $P_{t,\infty}$, h_t, and T%, expressions for the edge velocity gradient, stagnation pressure, density, and viscosity are required. Applying Euler's equation and assuming a modified Newtonian pressure distribution, the velocity gradient assumes the form

$$\frac{du_e}{dx} = \frac{8^{1/2}}{D}\sqrt{g_0 \frac{P_e}{\rho_e}\left(1 - \frac{P_\infty}{P_e}\right)} \tag{27}$$

The stagnation pressure P_e is given by[25]

$$P_e/P_\infty \simeq 0.95u_\infty^2/(g_0 \Re t) = 0.95\gamma M_\infty^2 \tag{28}$$

Given the stagnation pressure and enthalpy, the density and viscosity behind the shock can be computed. The wall enthalpy assumes the form[25]

$$h_w = t_w[0.234 + 0.01(t_w/1000)] \tag{29}$$

for $t_w < 4000°$R.

Wall Fluxes

The Nusselt number for heat transfer is defined as

$$Nu_{D,e} = \dot{q}_c'' D/\mu_e Pr_e^{-1}(h_w - h_e) \tag{30}$$

where e denotes the edge of the boundary layer. The preceding expression can be rewritten as

$$\frac{Nu_{D,e}}{(Re_{D,e})^{1/2}} = \sqrt{2}C_w \frac{Pr_w^{-1}}{Pr_e^{-1}} \frac{1}{(1-H_w)} \frac{\partial H}{\partial \eta}\bigg|_w \tag{31}$$

Similarly, a skin friction function defined by

$$\frac{C_f}{2}\frac{x}{D}(Re_{D,e})^{1/2} = \sqrt{2}C_w \frac{\partial^2 f}{\partial \eta^2}\bigg|_w \tag{32}$$

can be obtained from the definition of the skin friction coefficient

$$C_f/2 = \tau_w/\rho_e u_e^2 \tag{33}$$

It is also common practice to define a heat-transfer Nusselt number that is based on wall conditions and streamwise coordinate, $Nu_{x,w}$, which is related to $Nu_{D,e}$ as follows

$$Nu_D/\sqrt{Re_D} = Nu_x/\sqrt{Re_x} \tag{34}$$

$$\frac{Nu_{x,w}}{(Re_{x,w})^{1/2}} = \frac{Nu_{D,e}/(Re_{D,e})^{1/2}}{(Pr_w^{-1}/Pr_e^{-1})C_w^{1/2}} \tag{35}$$

Method of Solution

Quasilinearized forms of Eqs. (18-20) were reduced to coupled sets of algebraic equations by means of finite-difference methods, the resulting algebraic problem being solved iteratively until a prescribed convergence criterion was satisfied. Second-order-correct differencing of the η derivatives, in terms of three-point central difference analogs, was made possible by replacing Eq. (18) with the second-order system

$$g = df/d\eta$$

$$\frac{d}{d\eta}\left(C_{\text{eff}}\frac{dg}{d\eta}\right) + f\frac{dg}{d\eta} + \beta\left[\frac{\rho_e}{\rho} - g^2\right] = 0$$

Nonlinear terms, with the exception of (weak) nonlinearities incurred by variable property effects, were linearized about previous iterates, e.g.

$$f\frac{dg}{d\eta} \cong (f^0 + Rf)\frac{d}{d\eta}(g^0 + \Delta g) = f^0\frac{dg}{d\eta} + \frac{dg^0}{d\eta}f - f^0\frac{dg^0}{d\eta}$$

The resulting algebraic problem assumed the form

$$C_i\phi_i = A_i\phi_{i+1} + B_i\phi_{i-1} + S_i \qquad (i = 2,3,\ldots,IMX)$$

or, equivalently

$$\phi_i = A_i^*\phi_{i+1} + B_i^*$$

where C_i, A_i, and B_i are 4-4 coefficient matrices, and ϕ_i, S_i are 4-long column vectors. Although in principle the preceding matrix problem can be solved directly for each successive iterate of ϕ_i by means of successive substitution techniques, it proved convenient to solve the overall problem as follows: 1) construct initial distributions for f_i, g_i, H_i, and Q_i; 2) update variable properties; 3) solve iteratively the 2-2 matrix problem for f_i and g_i; 4) advance the algebraic problem for H_i; 5) solve iteratively the algebraic problem for Q_i; and 6) repeat steps 2-5. Convergence was assumed when successive iterates for the dependent-variable distributions differed by less than 0.01%. To promote numerical accuracy, a geometrical progression of mesh-spacings

$$(\eta_{i+1} - \eta_i) = \alpha(\eta_i - \psi_{i-1}),\ \alpha > 1$$

was introduced and numerical experiments performed to determine the truncation errors in wall fluxes. Using 61 node-points, with

$$(\eta_{IMX+1} - \eta_{IMX})/(\eta_2 - \eta_1) \cong 100$$

the absolute error in the reported results is judged to be less than 1%.

Results and Discussion

Laminar Flow ($T=0$)

The credibility of the numerical solutions was established by performing calculations under laminar flow conditions ($T=0$) and comparing selected results for the effect of the problem parameters on laminar heat transfer with previous investigations. In Table 1, it is seen that the present results for $Nu_w/Re_w^{1/2}$ differ from the well-known correlations of Fay and Riddell[1] and Cohen[26] by no more than 6.5 and 3.8%, respectively, over the given ranges of H_w and t_w. As expected, $Nu_w/Re_w^{1/2}$ decreases with decreasing H_w, for given t_w, because of reductions in the magnitude of the edge pressure gradient via reductions in ρ_e/ρ. (In the limit of extremely high t_e, or h_e, $Nu_w/Re_w^{1/2}$ approaches the flat-plate result for a zero-pressure-gradient flow.) Of further interest is the less sensitive variation in $Nu/Re^{1/2}$, based on edge conditions, with H_w.

Turbulent Flow ($T>0$)

Results were obtained for stagnation-region heat and momentum transfer to axisymmetric bodies in a turbulent environment. The results are reported in two different forms. First, heat-transfer enhancement is reported for a wide range

of specific freestream and wall conditions: Mach number (4-10), total temperature (2000°-6000°R), freestream intensity of turbulence (0-7%), freestream total pressure (35.0 and 70.0 atm), and wall temperature (540°-2500°R). A spherical model, 1.0 in. diam, was considered. Secondly, results for heat- and momentum-transfer enhancement are reported in terms of the dimensionless edge kinetic energy of turbulence and the enthalpy ratio across the boundary layer. In this latter form, freestream and wall conditions, as well as those behind the normal shock, are absorbed in the parameters Q_e and H_w, and a simple engineering correlation for the heat-transfer enhancement then could be obtained.

The numerical constants involved in the turbulence scheme (C_μ, A_μ, C_D, and A_D) were taken as 0.2, 0.35, 0.224, and 0.112, respectively. The turbulent Prandtl numbers Pr_h and Pr_q both were taken as 0.9.

Results in Terms of M_∞, $P_{t,\infty}$ t_t, T%, and t_w

Figure 1 displays plots of heat-transfer enhancement Nu/Nu_0 vs intensity of turbulence for different freestream Mach numbers. It is seen that Nu/Nu_0 increases monotonically with increasing T simply because of turbulent augmentation of the transfer process. As expected, heat transfer to the wall approaches the expected turbulence-free value (laminar value) as $T \to 0$. Figure 1 also demonstrates the strong dependence of Nu/Nu_0 on freestream Mach number. For example, at $T = 4\%$, heat-transfer enhancement increases from 4% to 68% on reducing M_∞ from 10 to 4 ($P_{t,\infty} = 70$ atm, $t_t = 3000°$R, and $t_w = 540°$R). This strong dependence on Mach number is due to physical property effects. The dimensionless edge kinetic energy of turbulence Q_e is a strong function of the gas density behind the shock, as can be seen from Eq. (23). For example, at $T = 5\%$, $P_{t,\infty} = 70$ atm, $t_t =$ 3000°R, and $t_w = 540°$R, Q_e assumes the values 2367.4, 582.4, 176.1, and 62.8 at $M_\infty = 4$, 6, 8, and 10, respectively. These reductions in Q_e are due primarily to decreases in ρ_e.

Figure 2 reports the effects of edge total temperature on Nu/Nu_0, which decreases with increasing t_t. The contribution of the turbulent fluctuations to the transfer process is less pronounced at higher temperatures because of strong reductions in eddy viscosity via density, which decreases with increasing enthalpy. Figure 3 demonstrates the increased turbulent enhancement to wall heat transfer at higher freestream total pressures, where now the turbulent contribution to the transfer process increases with increasing fluid density.

The effects of t_w on Nusselt number and heat-transfer enhancement are presented in Table 2a, where it is seen that increases in wall temperature, or H_w, lead to higher values of $Nu_w/(Re_w)^{1/2}$. Near the wall, the pressure gradient effect just discussed is more pronounced, leading to higher $Nu_w/(Re_w)^{1/2}$. (Recall that this source effect can be produced by lowering the edge total temperature.) It is to be noted that

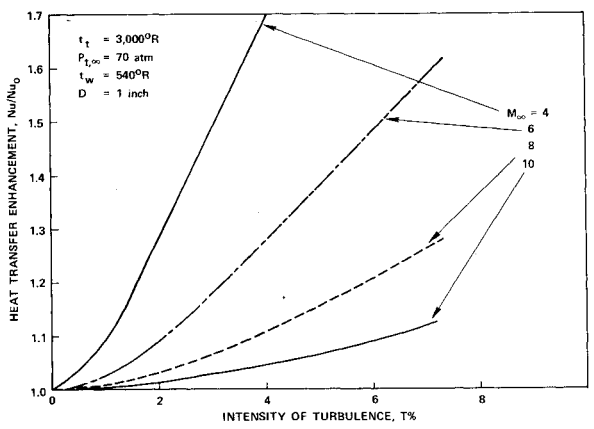

Fig. 1 Effect of Mach number on heat-transfer enhancement.

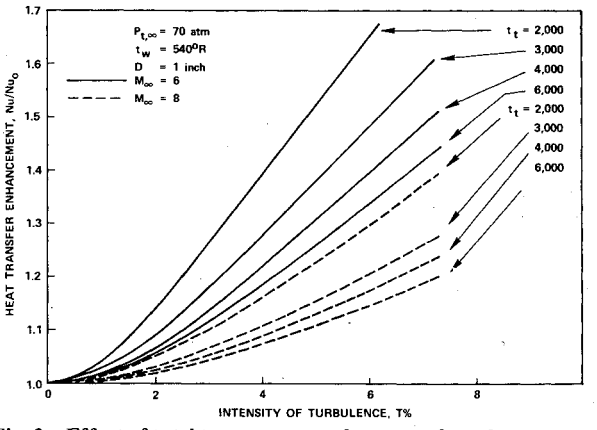

Fig. 2 Effect of total temperature on heat-transfer enhancement.

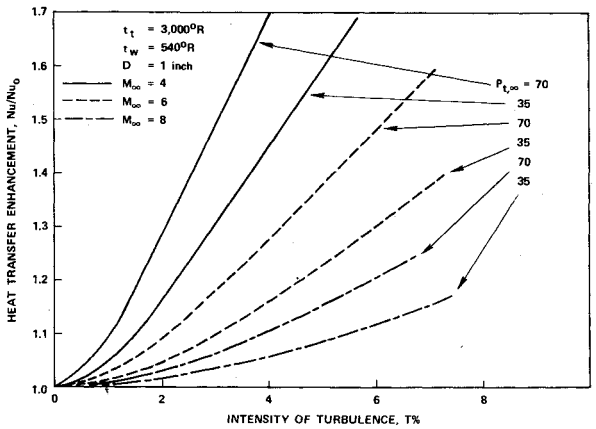

Fig. 3 Effect of freestream total pressure on heat-transfer enhance ment.

increasing the wall temperature leads not only to an increase in the heat-transfer enhancement but also to an increase in the laminar $Nu_w/(Re_w)^{1/2}$. On the other hand, the effect of wall temperature on $Nu_e/(Re_e)^{1/2}$ is reversed. Increases in t_w (or H_w) lead to reductions in $Nu_e/(Re_e)^{1/2}$ because of decreases in C_{eff} which outweight the effects of ρ_e/ρ.[27,28]

Results in Terms of Q_e and H_w

It was shown earlier that heat- and momentum-transfer enhancement can be expressed in terms of two parameters: the boundary-layer edge dimensionless kinetic energy of turbulence Q_e, and the wall-to-freestream (or total) enthalpy ratio H_w. It also was shown that freestream conditions and those behind the normal shock can be absorbed in these parameters, enabling simple engineering correlations for turbulent enhancement to the transfer process.

Table 2b gives a broad range of values of Nu/Nu_0 and $C_f/C_{f,0}$ in terms of Q_e(100-10,000) and H_w(0.9-0.1). It is seen that increasing Q_e increases monotonically heat- and momentum-transfer enhancement because of the turbulent contribution to the transfer process. Higher values of Q_e correspond to higher freestream turbulent velocity fluctuations and stagnation density, or lower stagnation viscosity and velocity gradient. Higher air density ρ_e corresponds to lower freestream Mach number and higher total pressure. On the other hand, a decrease in ρ_e and an increase in μ_e, which can be effected via increased total enthalpy or temperature, will reduce the value of Q_e. A lower velocity gradient corresponds to lower freestream Mach number or larger model diameter. It has been determined that the effect of wall temperature on Nu/Nu_0 and $C_f/C_{f,0}$, over the range of wall temperatures considered, is small and can be neglected. For example, the heat-transfer enhancement for $t_w = 1500°$F was

Table 2 Effects of problem parameters on heat- and momentum-transfer enhancement

a) $M_\infty = 8$, $t_t = 3000°R$, $P_{t,\infty} = 70$ atm

	$t_w = 540°R$			$t_w = 1500°R$			$t_w = 2500°R$		
$T\%$	$\frac{Nu_w}{(Re_w)^{1/2}}$	$\frac{Nu_e}{(Re_e)^{1/2}}$	$\frac{Nu}{Nu_0}$	$\frac{Nu_w}{(Re_w)^{1/2}}$	$\frac{Nu_e}{(Re_e)^{1/2}}$	$\frac{Nu}{Nu_0}$	$\frac{Nu_w}{(Re_w)^{1/2}}$	$\frac{Nu_e}{(Re_e)^{1/2}}$	$\frac{Nu}{Nu_0}$
0	0.524	0.756	1.00	0.594	0.726	1.00	0.668	0.692	1.00
1	0.528	0.762	1.01	0.600	0.734	1.01	0.676	0.701	1.01
2	0.539	0.779	1.03	0.617	0.754	1.04	0.696	0.722	1.04
3	0.556	0.804	1.06	0.642	0.784	1.08	0.726	0.753	1.09
4	0.578	0.835	1.10	0.672	0.821	1.13	0.762	0.790	1.14
5	0.603	0.872	1.15	0.706	0.863	1.19	0.802	0.831	1.20
6	0.631	0.911	1.20	0.742	0.907	1.25	0.844	0.875	1.26
7	0.659	0.952	1.26	0.779	0.952	1.31	0.887	0.920	1.33

b) $t_w = 540°R$

	$H_w = 0.9$		$H_w = 0.5$		$H_w = = 0.1$	
Q_e	$\frac{Nu}{Nu_0}$	$\frac{C_f}{C_{f,0}}$	$\frac{Nu}{Nu_0}$	$\frac{C_f}{C_{f,0}}$	$\frac{Nu}{Nu_0}$	$\frac{C_f}{C_{f,0}}$
100	1.12	1.04	1.11	1.05	1.09	1.05
250	1.26	1.09	1.23	1.12	1.19	1.12
500	1.42	1.16	1.38	1.20	1.32	1.20
1,000	1.64	1.26	1.59	1.32	1.51	1.32
2,000	1.94	1.41	1.88	1.49	1.78	1.49
4,000	2.33	1.61	2.25	1.72	2.13	1.73
6,000	2.61	1.76	2.53	1.89	2.38	1.91
8,000	2.84	1.88	2.74	2.03	2.58	2.05
10,000	3.03	1.99	2.93	2.15	2.76	2.18

found to be within 2.5% of that for $t_w = 540°R$. Therefore, for engineering purposes, the magnification in heat and momentum transfer owing to turbulence in the freestream is a function only of Q_e and H_w. Although $t_w = 540°R$ in Table 2b, the results can be used at higher wall temperatures.

Predictions in Arc-Heated Jet Environments

In attempting to quantify freestream turbulence effects on null-point calorimetric stagnation heat-transfer

Table 3 Flow conditions

Nozzle	Exit Mach number	Bulk enthalpy, Btu/lbm	Probe stagnation pressure, atm
1 (contoured)	3.1 ($D_e = 2.39$ in.)	2500	22.5
2 (conical)	3.9 ($D_e = 4.5$ in.)	2200	5.8
3	2.3	2200	28.1

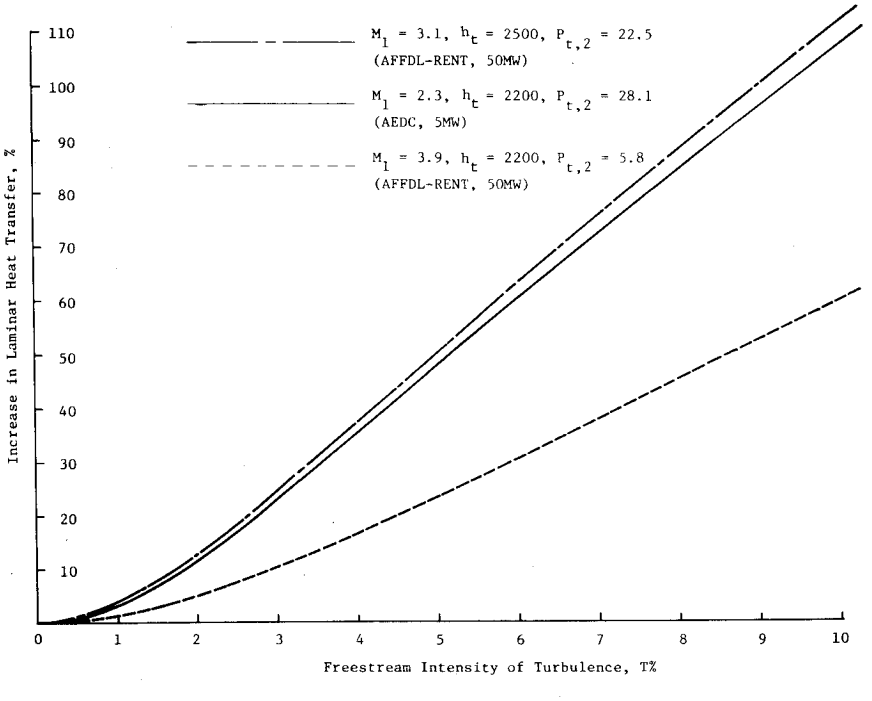

Fig. 4 Error in values of inferred enthalpies due to freestream turbulence.

measurements, i.e., to quantify the magnitude of the errors in values of inferred enthalpies, the flow conditions shown in Table 3 were considered. Flow conditions for nozzles 1 and 2 were taken from a test series conducted at the Re-Entry Nose Tip (RENT) test leg of the 50-MW facility at the Air Force Flight Dynamics Laboratory,[2] whereas the third nozzle flow conditions were taken from tests conducted in the 5-MW arcjet facility at Arnold Engineering Development Center.[29] It was assumed further that the bulk enthalpy, i.e., enthalpy obtained from an overall system energy balance, is the flow-correct enthalpy. Nose-radius null-point calorimeters of 0.25 in. were used in both tests.

Figure 4 depicts stagnation heat-transfer enhancement owing to turbulence in the freestream. It is seen that large errors can be incurred if turbulence effects are neglected. For example, a 6% turbulence intensity in the arc-heated jet results in a 60% increase in the measured heat transfer for nozzles 1 and 3 and a 30% increase for nozzle 2. (The lower increase for nozzle 2 is due to the higher Mach number and lower model stagnation pressure.)

Of particular relevance to the foregoing predictions are the experimental results for the test series. In all three cases, it was found that the *inferred* enthalpies were 60-90% higher than the (presumably correct) values obtained from overall energy balances.[2,29,30] Although precise measures of T for the test series are unavailable, values in excess of 6% are not unreasonable, and, in the case of the AFDL-RENT (50-MW) facility, values up to 12% would not be surprising because of the well-known characteristics of the arcjet in that facility.[2]

Summary and Conclusions

An analysis has been performed to predict heat- and momentum-transfer enhancement to axisymmetric bodies owing to turbulent velocity fluctuations in the freestream. Compressibility and variable property effects were included in the analysis. Results were obtained for both low- and high-enthalpy flows and show that freestream turbulence effects are more pronounced at higher total pressures and lower Mach numbers and enthalpies. The effects are less significant at low wall temperatures.

When applied to arc-heated jet facilities environments, the analysis predicts the discrepancies between inferred and measured bulk enthalpies over an appreciable range of intensity of turbulence. Additional study is needed to quantify the behavior of velocity fluctuations along a streamline passing through a shock and approaching the body surface.

References

[1]Fay, J. A. and Riddell, F. R., "Theory of Stagnation Point Heat Transfer in Dissociated Air," *Journal of the Aerospace Sciences,* Vol. 25, Feb. 1958, p. 73.

[2]Brown-Edwards, E. G., "Fluctuations in Heat Flux as Observed in the Expanded Flow from the RENT Facility Arc-heater," Air Force Flight Dynamics Lab., AFFDL-TR-73-102, 1973.

[3]Kestin, J., "The Effect of Free-Stream Turbulence on Heat Transfer Rates," *Advances in Heat Transfer,* Vol. 3, Academic Press, New York, 1966, pp. 1-32.

[4]Hsu, N. T. and Sage, B. H., "Thermal and Material Transfer in Turbulent Gas Stream: Local Transport from Spheres," *American Institute of Chemical Engineers Journal,* Vol. 3, Sept. 1957, pp. 405-410.

[5]Venezian, E., Crespo, M. J., and Sage, B. H., "Thermal and Material Transfer in Turbulent Gas Stream: One-Inch Spheres," *American Institute of Chemical Engineers Journal,* Vol. 8, July 1962, pp. 383-388.

[6]Gardon, R. and Akfirat, J. C., "Heat Transfer Characteristics of Impinging Two-Dimensional Air Jets," *Journal of Heat Transfer,* Vol. 88, Feb. 1966, pp. 101-108.

[7]Gardon, R. and Akfirat, J. C., "The Role of Turbulence in Determining the Heat Transfer Characteristics of Impinging Jets," *International Journal of Heat and Mass Transfer,* Vol. 8, Oct. 1965, pp. 1261-1272.

[8]Lavender, W. J. and Pei, D.C.T., "The Effect of Fluid Turbulence on the Rate of Heat Transfer from Spheres," *International Journal of Heat and Mass Transfer,* Vol. 10, April 1967, pp. 529-539.

[9]Gostkowski, V. U. and Costello, F. A., "The Effect of Free Stream Turbulence on the Heat Transfer from the Stagnation Point of a Sphere," *International Journal of Heat and Mass Transfer,* Vol. 12, Aug. 1970, pp. 1382-1386.

[10]Smith, M. C. and Kuethe, A. M., "Effects of Turbulence on Laminar Skin Friction and Heat Transfer," *The Physics of Fluids,* Vol. 9, Dec. 1966, pp. 2337-2344.

[11]Galloway, T.R., "Enhancement of Stagnation Flow Heat and Mass Transfer Through Interactions of Free Stream Turbulence," *American Institute of Chemical Engineers Journal,* Vol. 19, May 1973, pp. 608-617.

[12]Traci, R. M. and Wilcox, D. C., "Analytical Study of Freestream Turbulence Effect on Stagnation Point Flow and Heat Transfer," *AIAA Journal,* Vol. 13, July 1975, pp. 890-896.

[13]Wassel, A. T. and Denny, V. E., "The Effect of Free Stream Turbulence on Heat and Momentum Transfer to Axisymmetric Bodies," *Letters in Heat and Mass Transfer,* Vol. 3, May 1976, pp. 375-386.

[14]Sutera, S. P., Maeder, P. F., and Kestin, J., "On the Sensitivity of Heat Transfer in the Stagnation Point Boundary Layer to Free Stream Vorticity," *Journal of Fluid Mechanics,* Vol. 10, Aug. 1963, pp. 497-418.

[15]Sutera, S. P., "Vorticity Amplification in Stagnation Point Flow and its Effect on Heat Transfer," *Journal of Fluid Mechanics,* Vol. 21, March 1965, pp. 513-534.

[16]Weeks, T. M., "Influence of Freestream Turbulence on Hypersonic Stagnation Zone Heating," AIAA Paper 69-167, New York, Jan. 1969.

[17]Spalding, D.B., "Heat Transfer from Turbulent Separated Flows," *Journal of Fluid Mechanics,* Vol. 27, Jan. 1967, pp. 97-109.

[18]Wolfshtein, M., "The Velocity and Temperature Distribution in One-Dimensional Flow with Turbulence Augmentation and Pressure Gradient," *International Journal of Heat and Mass Transfer,* Vol. 12, March 1969, pp. 301-318.

[19]Wassel, A. T. and Catton, I., "Calculation of Turbulent Boundary Layers over Flat Plates with Different Phenomenological Theories of Turbulence and Variable Turbulent Prandtl Number," *International Journal of Heat and Mass Transfer,* Vol. 16, Aug. 1973, pp. 1547-1563.

[20]Van Driest, E. R., "On Turbulent Flow Near a Wall," *Journal of the Sciences,* Vol. 23, Oct. 1956, pp. 1007-1011.

[21]Spalding, D. B., "Monograph on Turbulent Boundary Layers," Chap. 2, Imperial College, Mechanical Engineering Dept., London, TR TWF/TN/33, 1967.

[22]Cohen, N. B., "Correlation Formulas and Tables of Density and Some Transport Properties of Equilibrium Dissociating Air for Use in Solutions of the Boundary Layer Equations," NASA TN D-194, 1960.

[23]Hansen, C. F., "Approximations for the Thermodynamic and Transport Properties of High Temperature Air," NACA TN 4150, 1958.

[24]Clutter, D. W. and Smith, A. M. O., "Solution of the General Boundary Layer Equations for Compressible Laminar Flow Including Transverse Curvature," Douglas Corp., Long Beach, Calif., Rept. LB-31099, 1963.

[25]Ohrenberger, J. T., "A Review and Applications of Stagnation Point and Laminar Boundary Layer Similar Solutions to Heat Transfer," Space Technology Laboratories, Inc., Redondo Beach, Calif., 6121-7506-KU-000, 1963.

[26]Cohen, N. B., "Boundary Layer Similar Solutions and Correlation Equations for Laminar Heat Transfer Distribution in Equilibrium Air at Velocities up to 41,000 ft/sec," NASA TR R-118, 1961.

[27]Wortman, A. and Mills, A. F., "Highly Accelerated Compressible Laminar Boundary Layer Flows with Mass Transfer," *Journal of Heat Transfer,* Vol. 93, Aug. 1971, pp. 281-289.

[28]Landis, R. B. and Mills, A. F., "The Calculation of Turbulent Boundary Layers with Foreign Gas Injection," *International Journal of Heat and Mass Transfer,* Vol. 15, Oct. 1972, pp. 1905-1932.

[29]Smith, R. T., MacDermott, W. N., and Filtinan, T. L., "A Transient Enthalpy Probe for the Calibration of High Heat Flux Ablation Facilities," Arnold Engineering Development Center, AEDC-TR-74-116, 1975.

[30]Hoshizaki, H., Chou, Y.S., Kulgein, N.G., and Meyer, J.W., "Critical Review of Stagnation Point Heat Transfer Theory," Air Force Flight Dynamics Lab., AFFDL-TR-75-85, 1975.